

# Study of the supramolecular chiral assembly of *meso*-“C-glucoside”-porphyrin derivatives in aqueous media†

Donato Monti,<sup>\*a</sup> Mariano Venanzi,<sup>a</sup> Emanuela Gatto,<sup>a</sup> Giovanna Mancini,<sup>b</sup> Alessandro Sorrenti,<sup>b</sup> Petr Štěpánek<sup>c</sup> and Pavel Drašar<sup>\*c</sup>

Received (in Durham, UK) 17th April 2008, Accepted 1st July 2008

First published as an Advance Article on the web 26th August 2008

DOI: 10.1039/b806515b

The solvent driven self-aggregation studies of several *meso*-“C-glycoside”-porphyrin derivatives have been carried out, showing the effect of bulk solvent properties, and of the structure of the molecular framework, on the supramolecular chirality of the mesoscopic final architectures.

## Introduction

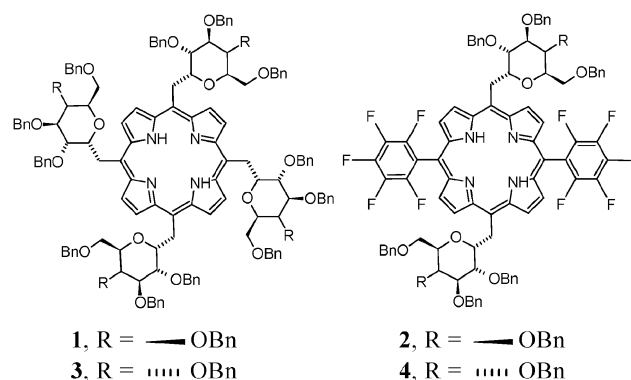
“Supramolecular Chirality” constitutes, undoubtedly, one of the most fascinating issues of Supramolecular Chemistry,<sup>1</sup> allowing the transfer of asymmetry information (*i.e.* sensing, induction, amplification) within multimolecular systems *via* noncovalent interactions. This has profound implications, for example, in the field of nanotechnology,<sup>2</sup> and in the construction of sensor devices with stereoselective properties.<sup>3</sup> In particular, the evolution of chiral porphyrin systems at a supramolecular level mainly relies, among others, on the aggregation of achiral porphyrin platforms on chiral templates, such as DNAs, RNA, and other natural or synthetic polymers upon electrostatic interaction,<sup>4</sup> by anion-controlled assemblies,<sup>5</sup> on chiral ligand coordination,<sup>6</sup> or by directional stirring.<sup>7</sup> Some recent examples of the achievement of chiral porphyrin films upon symmetry breaking at air/liquid interfaces, by Langmuir–Sheafer (LS) deposition protocols, have been reported,<sup>8</sup> with the chirality of the films, occurring in a random fashion. The “reading-out” process, *i.e.* the critical step in the transfer of the stored molecular information, is onset by the presence of peculiar functional groups (*i.e.* *chirophores*),<sup>9</sup> exerted *via* non-covalent interactions, such as hydrogen bonding, electrostatic forces,  $\pi$ – $\pi$  and other dispersion forces, or hydrophobic effect. Our approach pursued so far, relies on the functionalisation the periphery of the porphyrin macrocycle, by a charged, chiral group, that induces the formation of supramolecular systems expressing elements of chirality.<sup>10</sup>

Recently, we published the synthesis and solvent driven self-aggregation studies of *meso*-“C-glycoside”-porphyrin derivatives<sup>11</sup> (**1** and **2**, Scheme 1) showing the effect of the structure of the molecular framework on the aggregation properties, in terms of morphology and chirality of the mesoscopic final

structures. In this work, we wish to report on the aggregation properties of porphyrin derivatives **3** and **4** (Scheme 1). These derivatives are structural analogues of previously reported ones (Scheme 1), differing from the configuration at one carbon of the “sugar” units from “D-galacto” to “D-gluco”.<sup>‡</sup> The aggregation properties of these derivatives, in terms of concentration, solvent composition, and effect of the ionic strength were studied, evidencing a marked influence of the structural change, *i.e.* epimerization, on the aggregation properties and morphology of the final structures. The results will be extremely important for getting additional insights about the phenomena involved in the chiral supramolecular aggregation of such an important class of chromophores. Moreover, this would enable the building of complex porphyrin architectures in which the final supramolecular chirality can be tuned *ad hoc*.

## Results and discussion

Porphyrin derivatives **3**, and **4** were obtained by following the procedures recently reported in our previous paper.<sup>11</sup> Two basic strategies were used for their synthesis: one, leading to a porphyrin type with all four *meso*-positions substituted with identical ligand (type A), relies on direct cyclization of “sugar” aldehydes with pyrrole, whereas the second, based on sequential construction from the dipyrromethane precursors, yields to porphyrin derivatives with 5,15-*meso*-substitution pattern (type B). The compounds used in this study differ on the number of the “C-D-gluco” moieties, namely **3** possesses four



Scheme 1 Porphyrins employed in the aggregation studies.

<sup>a</sup> Department of Chemical Technologies, University of Rome “Tor Vergata”, Via, della Ricerca Scientifica, 1, 00133 Rome, Italy. E-mail: monti@stc.uniroma2.it; Fax: +39 0672594328; Tel: +39 0672594738

<sup>b</sup> IMR-CNR, c/o Department of Chemistry, University of Rome “La Sapienza”, P.le A. Moro, 5, 00185 Rome, Italy

<sup>c</sup> ICT Prague, Technická 5, CZ-16628 Praha, Czech Republic. E-mail: Pavel.Drasar@vscht.cz; Fax: +420 220 444 422; Tel: +420 220 444 283

† Electronic supplementary information (ESI) available: UV-visible plots, aggregation curves, kinetic profiles, RLS and CD spectra of porphyrin derivatives **2**, **3** and **4**. See DOI: 10.1039/b806515b

“D-glucosyl” groups, whereas **4**, is characterised by the presence of two “D-glucosyl” and two pentafluorophenyl moieties, in mutual *trans* position. These differences should infer different electronic and steric properties that should bring different features in terms of solubility and self-aggregation properties. These tetrapyrrolic macrocycles show good solubility in either chlorinated and polar aprotic solvents such as DMSO, DMF, MeCN, and EtOH. The relative UV-visible spectra, in either MeCN or in EtOH, at  $\mu\text{M}$  concentration, show a narrow Soret band ( $\lambda_{\text{max}}$  419 and 416 nm, in chloroform, for **3** and **4**, respectively) indicating the solubilisation of the chromophores in monomeric form. The hypsochromic shift of porphyrin derivative **4** is safely ascribable to the electron withdrawal effect of  $\text{C}_6\text{F}_5$  moieties.

The presence of these polar groups infers a peculiar amphiphilic character to the title macrocycles, resulting in some degree of solubility in organic/water solvent mixtures. The aggregation properties were studied in two different bulk solvents, namely acetonitrile–water and ethanol–water mixtures, at micromolar concentration, unless otherwise stated. The overall behaviour is dependent on the intimate nature of the macrocycle structures, *i.e.* nature and number of substituents, as discussed in detail in the following sections. Both tetrapyrrolic platforms are in monomeric form in pure organic solvents, the aggregation process is onset on going toward more water rich mixtures, by hydrophobic effects ( $\pi$ – $\pi$  and dispersion forces), as well as, as recently recognized by Waters and co-workers, by specific carbohydrate– $\pi$  interactions.<sup>12</sup> It has been recognised that the carbohydrate effect is exerted by the C–H group of the  $\alpha$ -face of the sugar moiety. This interaction may be more important than hydrogen bonding in aqueous or polar media, and is of greater importance in protected sugars, owing to a lower enthalpy of desolvation.

### Aggregation in acetonitrile–water mixtures

Aggregation studies of derivatives **3** and **4** in acetonitrile–water mixtures show unusual differences, with respect to the previously published “D-galactosyl”-porphyrin congeners (**1** and **2**, Scheme 1).<sup>11</sup> Namely, in the case of porphyrin derivative **3**, aggregation occurs at water composition  $\geq 40\%$ , whereas in the case of the derivative **4**, the “critical aggregation solvent composition” (*casc*) is  $\geq 45\%$ . In both of the cases the aggregation results in coupled, slightly blue-shifted, Soret bands, indicating the formation of H-type porphyrin self-aggregates.<sup>13§</sup>

‡ Authors deliberately use the terms “D-galactosyl”, “D-glucosyl”, and “C-glycoside” terms, knowing it is not of rigorous carbohydrate nomenclature. “C-glycoside” is a common name of a sugar derivative in which an oxygen atom of the glycosidic bond is replaced by a methylene group. However, using rigorous IUPAC carbohydrate or heterocyclic names would make the whole text rather complicated (see, for example: Y. Chapleur, *Carbohydrate Mimics: Concepts & Methods*, Wiley-VCH Verlag GmbH, 1998).

§ At a peculiar intermediate solvent composition (*i.e.* 60–70% MeCN) a “macroaggregation” effect of the monomers is observed, witnessed by the occurrence of a strong opalescence of the solutions. This phenomenon is reversible, and diminishes on storing the samples (days–week). Conversely, in mostly-water media, clear, perfectly transparent solutions are always obtained.

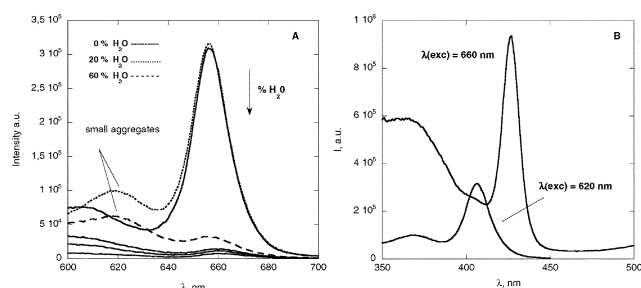


**Fig. 1** Fluorescence (A) and excitation (B) spectra of **3** ( $3.4 \mu\text{M}$ ) in different MeCN– $\text{H}_2\text{O}$  mixtures.

The corresponding fluorescence studies ( $\lambda_{\text{exc}} = 518 \text{ nm}$ ;  $\lambda_{\text{max}} = 660 \text{ nm}$ ) indicate that the aggregation occurs, expectedly, with a quenching of the emission intensity indicating the formation of strongly electronically coupled, non-radiative, porphyrin aggregates. It is worth noting that the drop in signal emission occurs at the same solvent composition found by UV-visible techniques, safely confirming the occurrence of the aggregation phenomena. Interestingly, in the case of derivative **3**, at MeCN-rich solvent composition (*i.e.* 80–60% MeCN), a new weaker emission feature, at  $\lambda_{\text{max}} = 620 \text{ nm}$ , is evidenced (Fig. 1(A)). The corresponding excitation spectra, carried out in order to acquire information on the “parent chromophore absorption” responsible for the emission signals, indicate that the principal, intense fluorescence emission (660 nm) arises from the porphyrin in monomeric form, whereas the weaker emission at 620 nm is due to blue-shifted porphyrin aggregates ( $\lambda = 406 \text{ nm}$ ), probably dimers,<sup>14</sup> or other pre-aggregated oligomeric structures (Fig. 1(B)). This is further corroborated by resonance light scattering spectroscopy (RLS) studies, that showed no enhanced scattering of the solution, indicating that the above weakly fluorescent “proto-aggregate” structures should be composed of a number of units smaller than 25.<sup>15</sup> On increasing the water proportion (MeCN  $\leq 50\%$ ), the emission of the oligomeric species disappears, due to extensive aggregation. The RLS spectra consequently show intense resonating scattering signals in the Soret band region (*i.e.* *ca.*  $10^7$ – $10^8$  cps), confirming the aggregation of the macrocycles. In the case of porphyrin derivative **4**, the presence of such intermediate oligomeric species could not be detected.

Kinetic studies on the self-aggregation of the above macrocycles, indicated a fast aggregation process above the *casc* (*i.e.*  $>40$  and  $>45\%$  water, for **3** and **4**, respectively) completed within the time of mixing, that could not be followed by conventional spectrophotometric means. At lower water proportion (*i.e.* 85% MeCN–15%  $\text{H}_2\text{O}$ ), the aggregation process can be promoted by ionic strength, but the results have been found to be severely affected by scattering effects, and by precipitation of salts from the solution with time, or even separation of the organic and aqueous phases at higher salt concentration. Detailed kinetic studies, however, can be carried out in more “halophilic” aqueous media, such as EtOH– $\text{H}_2\text{O}$  solvent mixtures (see next section).

### Aggregation in ethanol–water mixtures

Detailed, aggregation studies, in terms of aggregates morphology and kinetic behaviour, could be carried out in ethanol–water

mixtures, owing to the better solubility of the porphyrin substrates **3** and **4** at micromolar concentration, in the new bulk solvent conditions.

Preliminary aggregation curves carried out on the porphyrin derivatives **3** and **4** show similar behaviour with respect to those performed in MeCN–water mixtures, in terms of coupled, slightly hypsochromically-shifted Soret bands, indicating alike morphology of the aggregates. Noteworthy, no opalescence of the solutions can be observed upon going from 100% ethanol to 100% water solvent composition. Peculiarly, some opalescence occurs after very prolonged standing (>5 days), for the 80% EtOH solvent mixture for both porphyrin derivatives. Parallel experiments, carried out on the “D-galacto”-porphyrin derivative **2**, showed that the aggregation in EtOH–H<sub>2</sub>O mixtures occurs with the formation of species featuring a large broadening, and red shift of the Soret band, similar to that formerly observed for this macrocycle in MeCN–H<sub>2</sub>O media (ESI,† Fig. S1). This implies that the differences observed in the spectroscopic changes are not dependent on the solvent used, but can be safely ascribed on the different configuration of the glycoside moieties.

The relative spectra, and the corresponding aggregation profiles, are reported in Fig. 2. The bis-C<sub>6</sub>F<sub>5</sub>-derivative **4** shows critical solvent composition at somewhat higher water proportion, with respect to the tetra-“C-D-gluco” derivative **3** congener (*i.e.* 85% vs. 80%). This could be explained in terms of high polarity conferred by the C<sub>6</sub>F<sub>5</sub> moieties to the macrocycle. Also in this case, kinetic studies on the self-aggregation of the title macrocycles, indicated a fast aggregation process above the *casc* (*i.e.* >15 and >20% of water, for **3** and **4**, respectively) that could not be followed by conventional UV-visible spectroscopy. Before these values, however, the aggregation process could be followed by spectroscopic means. The kinetics of aggregation can be carried out by conventional hand-mixing techniques, and can be conveniently followed by monitoring the decrease of Soret band intensity with time. The

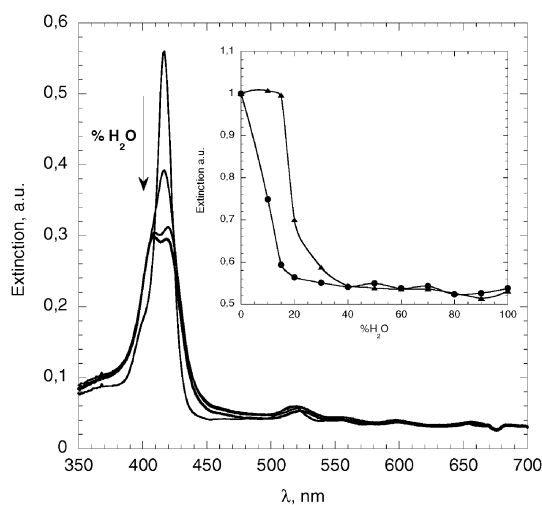


**Fig. 2** Spectral variations of **4** (3.4 μM) in EtOH–water mixtures, on increasing water proportion. Inset: corresponding aggregation profiles for **3** ( $\lambda = 419$  nm, full circles) and **4** ( $\lambda = 416$  nm, triangles).

experimental data points can be nicely fit by a so-called “stretched exponential” equation (eqn (1)).<sup>16</sup>

$$Ext = Ext_0 + \Delta Ext[1 - \exp(-(kt)^n)] \quad (1)$$

In this equation  $Ext_0$  represent the initial extinction at  $t = 0$ ,  $\Delta Ext = Ext_\infty - Ext_0$  is the difference between the initial extinction value ( $t = 0$ ) and that at  $t = \infty$ ,  $k$  is the kinetic rate constant, and  $n$  is the aggregation growth factor, related to the mean value of binding sites available for aggregate growth process. This equation is of validity in the case of mono-dispersed systems,<sup>16</sup> in which large clusters are formed by interaction between initial smaller clusters (seeds) and monomers. In this case, known as diffusion limited aggregation (DLA), the  $n$  factor is required to be <1. Notable examples are reported in the aggregation of charged cyanine dyes on charged polymeric templates, such as poly(vinylsulfonate),<sup>17</sup> or in our previous work.<sup>11</sup>

The chosen solvent composition corresponded to 85% ethanol. Derivative **3**, showed very low aggregation rates, which could be calculated with appreciable accuracy, only at higher porphyrin bulk concentration. More detailed studies could be carried out in the case of **4**, featuring substantially higher aggregation rates that are dependent on the initial porphyrin concentration. The higher rates observed could be due to the presence of the pentafluorophenyl groups in *meso* positions, which promote the sugar– $\pi$  interaction. The results are summarised in Table 1.† The aggregation has been found to be promoted by ionic strength (*i.e.* NaBr), at the same solvent composition, in the case of both porphyrin derivative **3** and **4**, in EtOH–H<sub>2</sub>O (85 : 15 v/v). Noteworthy, in these cases the aggregation occurs with formation of species with different

**Table 1** Kinetic parameters ( $k$ ,  $n$ ) for the aggregation of porphyrin **3** and **4**, in EtOH–H<sub>2</sub>O (85 : 15 v/v) in various bulk conditions<sup>a</sup>

| Entry                    | Porphyrin            | [NaBr]/M           | $k/s^{-1}$           | $n$  |
|--------------------------|----------------------|--------------------|----------------------|------|
| <b>[3]<sup>b</sup>/M</b> |                      |                    |                      |      |
| 1                        | $3.4 \times 10^{-6}$ | 0.000 <sup>c</sup> | $1.2 \times 10^{-6}$ |      |
| 2                        |                      | 0.0196             | $3.3 \times 10^{-5}$ | 0.32 |
| 3                        |                      | 0.0385             | $6.6 \times 10^{-5}$ | 0.43 |
| 4                        |                      | 0.0566             | $8.5 \times 10^{-5}$ | 0.42 |
| 5                        |                      | 0.0741             | $1.1 \times 10^{-5}$ | 0.38 |
| 6                        | $8.4 \times 10^{-6}$ | 0.0385             | $3.2 \times 10^{-4}$ | 0.46 |
| 7                        | $1.7 \times 10^{-5}$ | 0.000              | $3.2 \times 10^{-6}$ | 0.25 |
| 8                        |                      | 0.0385             | $4.8 \times 10^{-4}$ | 0.52 |
| <b>[4]<sup>d</sup>/M</b> |                      |                    |                      |      |
| 9                        | $3.4 \times 10^{-6}$ | 0.000              | $5.7 \times 10^{-6}$ | 0.35 |
| 10                       |                      | 0.000 <sup>c</sup> | $1.2 \times 10^{-5}$ |      |
| 11                       |                      | 0.0196             | $5.7 \times 10^{-4}$ | 0.17 |
| 12                       |                      | 0.0385             | $7.3 \times 10^{-4}$ | 0.18 |
| 13                       |                      | 0.0566             | $9.3 \times 10^{-4}$ | 0.14 |
| 14                       |                      | 0.0741             | $1.1 \times 10^{-3}$ | 0.16 |
| 15                       | $8.4 \times 10^{-6}$ | 0.0385             | $7.7 \times 10^{-4}$ | 0.21 |
| 16                       | $1.7 \times 10^{-5}$ | 0.0385             | $8.0 \times 10^{-4}$ | 0.23 |

<sup>a</sup> UV-visible spectroscopy,  $T = 298.0$  K. <sup>b</sup>  $\lambda = 419$  nm. <sup>c</sup> Extrapolated value at [NaBr] = 0.0 M. <sup>d</sup>  $\lambda = 416$  nm.

† The corresponding aggregation constant values, at 3.4 μM concentration, in 70% EtOH, are  $1.3 \times 10^{-6}$  and  $6.3 \times 10^{-5} s^{-1}$ , at 0.0, and 0.0385 M NaBr concentration, respectively (D. Monti and P. Drasar, unpublished results).

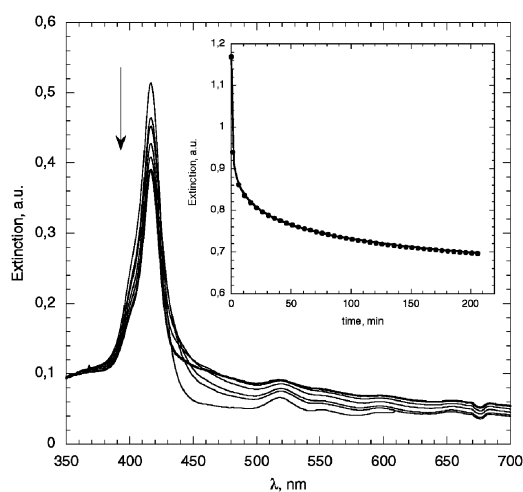


**Fig. 3** UV-visible spectral changes for the aggregation of **4** (3.4  $\mu\text{M}$ ) in EtOH–H<sub>2</sub>O (85 : 15 v/v) at [NaBr] = 0.0385 M with time,  $T$  = 298.0 K. Inset: corresponding kinetic profile, at  $\lambda$  = 416 nm.

morphology. In the case of derivative **4**, for example, the Soret band evolves with only an aspecific hypochromic effect (Fig. 3), whereas, for the *tetra*-“C-D-glucosyl” congener **3**, the spectroscopic features of the final aggregated species, are characterised by broadened B bands, red shifted by *ca.* 5–10 nm, with a drift of the baseline on going toward lower wavelengths, typical of severely scattered solutions (ESI,† Fig. S2). In all cases investigated, the final solutions presented some opalescence after prolonged standing, eventually resulting in some precipitation of porphyrin material, especially at high substrate and salt concentrations. Also in these latter cases, however, the spectral variations can be nicely fitted by a stretched exponential curve. A typical example is reported in Fig. 3, in which the close adherence of the experimental points to the calculated curve fit can be nicely observed. The calculated kinetic parameters are also reported in Table 1. From inspection of Table 1, it clearly emerges that the aggregation rates depend linearly on the ionic strength of the medium, as graphically depicted in Fig. 4. The *bis*-C<sub>6</sub>F<sub>5</sub> derivative **4**, also in this case, shows a substantial higher tendency to aggregation, with the apparent aggregation rate constant higher by *ca.* one order of magnitude with respect to that observed for **3**, besides an higher effect of the ionic strength, as indicated by the steeper slope of the corresponding  $k$  vs. [NaBr] plot. The kinetic profiles, defined by a stretched exponential decay curve, are characterized by an “initial burst”, followed by a slower final evolution. The corresponding aggregation factors “ $n$ ” are quite low (0.16–0.18) with respect to that featured by the *tetra*-“D-glucosyl” congener (0.34–0.42).

Quite surprisingly, the aggregation rates, performed at fixed ionic strength (*i.e.* NaBr = 0.0385 M), depend only marginally on the initial concentration of **4**, the observed rate constant values in fact, slightly increasing upon varying the initial porphyrin concentration within one order of magnitude.

A small increase in the aggregation factor “ $n$ ” is observed on increasing the porphyrin concentration. Moreover, it can be noted that the aggregation rates, obtained in absence of added salt, are lower than the  $k$  values obtained in the presence of salt, extrapolated to [NaBr] = 0.0 M. This finding indicates

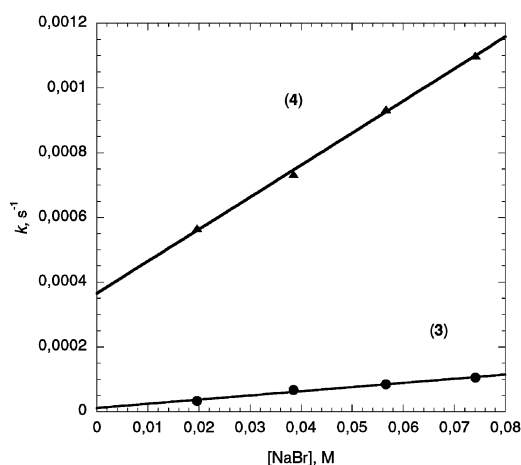


**Fig. 4** Dependence of the rate constant values  $k$ , on the ionic strength of the solution, for the aggregation of **3** (●) and **4** (▲) at 3.4  $\mu\text{M}$  porphyrin concentration, in EtOH–H<sub>2</sub>O (85 : 15 v/v) at 298 K.

a different intrinsic rate for the formation of the aggregates with different morphology. Notably, in the case of derivative **4**, these experimental findings are accompanied by a change in the aggregation factor  $n$ , which is quite higher in the *unpromoted* aggregation (*i.e.* 0.35 vs. 0.16, see Table 1). This would imply a change in the aggregation mechanism, from DLA, to DLCCA (diffusion limited cluster–cluster aggregation), as earlier reported for the case of specific ion-pairing effect on the cationic–anionic porphyrin interaction.<sup>18</sup> This issue is currently under investigation in our laboratories, and the results will be reported elsewhere.

Addressed RLS spectra, carried out at constant bulk porphyrin concentration (ESI,† Fig. S3), showed some differences in the intensities of the spectral features related to the aggregated species. In the case of the aggregation carried out in the presence of NaBr, the resulting bathochromically shifted aggregated species, gave rise to RLS features with higher intensity. Conversely, in the case of the aggregated structures with coupled, slightly hypsochromically shifted Soret band, obtained without added NaBr, the corresponding RLS features are of lower intensity. Such differences are accompanied by a corresponding higher extent of quenching of fluorescence emission. This holds for both **3** and **4** macrocycles. This would indicate either a higher degree of inter-chromophoric electronic coupling, steered by the higher ionic strength (hydrophobic effect) of the bulk media, or the formation of higher aggregates. Concomitant circular dichroism spectroscopy studies gave results that are more in line with this second hypothesis (*vide infra*).

### CD spectroscopic studies

We recently reported that the presence of a chiral functionality, on the molecular framework of amphiphilic porphyrin derivatives, steers the aggregation toward the formation of structures featuring supramolecular chirality.<sup>10,11</sup> CD spectra of **4**, for example, carried out in non-aggregative conditions (*i.e.* 100% EtOH), shows a positive band at  $\lambda_{\text{max}}$  = 417 nm ( $[\theta]$  =  $4.5 \times 10^4$  deg cm<sup>2</sup> dmol<sup>−1</sup>), due to the presence of the chiral appended group. Remarkably, on going to more



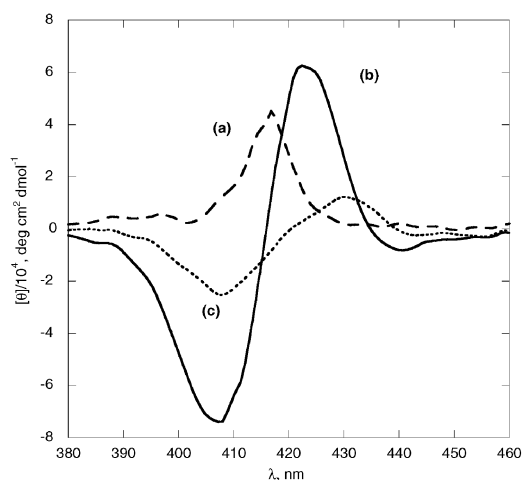


**Fig. 5** CD spectroscopic features of **4** (3.4  $\mu\text{M}$ ,  $T = 298\text{ K}$ ) in various bulk media: (a) 100% EtOH; (b) 40% EtOH; (c) EtOH 40%, NaBr 0.074 M.

water rich solvent mixtures (*i.e.* in EtOH 40%, see Fig. 5), in which the aggregation takes place, this spectral feature evolves into a more intense, positive, bisignate CD spectra with conservative features at  $\lambda(+)_\text{max} = 423\text{ nm}$  ( $[\theta] = 6.3 \times 10^4\text{ deg cm}^2\text{ dmol}^{-1}$ ) and  $\lambda(-)_\text{max} = 407\text{ nm}$  ( $[\theta] = -7.4 \times 10^4\text{ deg cm}^2\text{ dmol}^{-1}$ ), with a “crossover point” at 416 nm. This indicates that the presence of the sugar moieties triggers the aggregation toward the formation of electronically coupled porphyrin architectures, featuring supramolecular chirality, in which the porphyrin chromophores are held in mutual clockwise (+) chiral orientation. It is interesting to note that similar behaviour, in terms of intensity ( $\theta$ ) and  $\lambda_\text{max}$ , is observed in MeCN–H<sub>2</sub>O media (ESI,† Fig. S4). The same results have been found in the case of derivative **3**.

On the other hand, for aggregation carried out in the presence of added salts a strong decrease of the band intensities is observed, as reported for **4**, showing somewhat bathochromically shifted spectral features at  $\lambda(+)_\text{max} = 430\text{ nm}$  ( $[\theta] = 1.2 \times 10^4\text{ deg cm}^2\text{ dmol}^{-1}$ ) and  $\lambda(-)_\text{max} = 407\text{ nm}$  ( $[\theta] = -2.5 \times 10^4\text{ deg cm}^2\text{ dmol}^{-1}$ ), with a “crossover point” at 420 nm. This should imply that the aggregation occurs with the formation of supramolecular species in which the stereogenic molecular information is less effective, due to the shielding of the polar sugar moieties, by ion-dipole interaction with the sodium cations.<sup>19</sup>

Remarkably, these results show interesting differences with respect to those obtained for the formerly reported “D-galacto” congeners **1**, and **2**.<sup>11</sup> In this latter case coupled, bisignated negative bands were observed upon extensive water-promoted aggregation, with conservative features at  $\lambda(-)_\text{max} = 427\text{ nm}$  ( $[\theta] = -5.7 \times 10^4\text{ deg cm}^2\text{ dmol}^{-1}$ ) and  $\lambda(+)_\text{max} = 412\text{ nm}$  ( $[\theta] = 3.8 \times 10^4\text{ deg cm}^2\text{ dmol}^{-1}$ ), with a “crossover point” at 419 nm. This indicates the formation of aggregates in which the porphyrin units are held in mutual anticlockwise (–) orientation. This effect is certainly dependent on the stereochemical information brought by the sugar moieties, in which the configurational change at C4, occurring on going from “D-galacto” to “D-gluco” stereoisomers, steers a self-aggregation process with different overall stereochemistry, resulting in

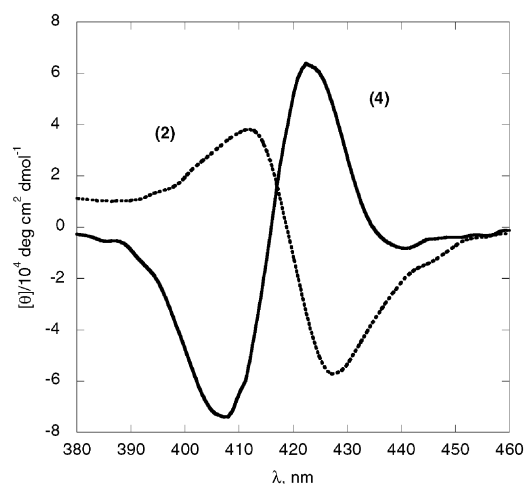


**Fig. 6** CD spectra of porphyrin derivatives **2** and **4**, in EtOH 40%.

aggregates with opposite supramolecular chirality, as shown in Fig. 6.†

This finding indicates that the overall supramolecular chirality of the aggregates can be effectively tuned by the configuration of the *ancillary* groups linked to the periphery of the porphyrin macrocycles. This would certainly constitute an important issue, not only from an academic point of view, but also for possible practical applications, such as the construction of biomimetic systems,<sup>20</sup> porphyrin-based molecular materials,<sup>21</sup> chiral molecular recognition,<sup>3,22</sup> and enantioselective catalysis.<sup>23</sup>

## Conclusions

The results obtained show the possibility of constructing porphyrin aggregates featuring supramolecular chirality, by linking sugar derivatives on the *meso*-position of the macrocycles. The aggregation properties, and the asymmetry of the supramolecular architectures can be finely modulated by changing the number of the appended groups, and by changing the configuration at one carbon unit of the sugar moieties. This issue, in which the chirality of a stereogenic centre is transferred into a complex supra-assembled structure, would have important application in the field of molecular materials, sensors, and asymmetric catalysis. Moreover, these systems in which the transfer of chiral information from a molecule to an assembly, *via* non-covalent interactions, bringing into these new architectures a new functionality, are of fundamental importance in the study of the origin of the homochirality<sup>24a,b</sup> and chiral amplification in biological and natural systems.<sup>24c</sup>

† The different CD properties featured by the “D-galacto” and “D-gluco” derivatives in non-aggregative conditions, would be also ascribed to the effect of different solvation of the sugar moieties on the *meso*-position of the porphyrin frameworks. In the case of the “D-gluco” group an optimal geometry can be reached, triggering the porphyrin–sugar coupling of the transition momenta. On the contrary, in the case of the “D-galacto” group, a different solvation would preferentially drive a different geometry, hampering the electronic coupling. For a discussion on the solvent effect on chirality induction, see refs. 6a,c and 10b.

## Experimental

### Preparation of porphyrin derivatives

Porphyrin derivatives were accomplished according to procedures described in our previous paper.<sup>11</sup>

### Aggregation studies

Solutions suitable for the aggregation studies were prepared as follows. Measured aliquots, of a millimolar stock solution in ethanol (15–150  $\mu$ L), were added to a measured amount of solvent in an 8 mL glass vial. To this solution the required amount of water were then added, to give 4.0 ml of resulting solution. A 3 mL portion was transferred in a quartz cuvette and the relative UV-visible spectra acquired. The corresponding absorbance vs. solvent composition (*i.e.* water%) plots indicate the critical aggregation solvent composition (*case*). Spectra were further acquired at different times in order to get indications on suitable solvent mixtures to be used for addressed kinetic experiments.

### Kinetic studies

Kinetic experiments were performed on a Perkin Elmer  $\lambda$ 18 Spectrophotometer equipped with a thermostating apparatus, by measuring the UV-visible spectroscopic changes (Soret B band) of porphyrin derivatives with time. Porphyrin aqueous solutions, suitable for kinetic studies, were prepared as follows. Measured aliquots, of a millimolar stock solution in ethanol (15–150  $\mu$ L), were added to a measured amount of ethanol, to give 0.600 ml of final solution. To this solution 3.400 ml of water were then added and the resulting 4.000 ml solution vigorously shaken. A suitable portion was rapidly transferred in a quartz cuvette and the relative UV-visible spectra acquired, with time. This procedure ensures a 85 : 15 H<sub>2</sub>O–EtOH (v/v) final solvent composition, with final porphyrin concentrations spanning the range  $(3.4\text{--}17.0) \times 10^{-6}$  M. Values of  $k$  were obtained by analysing the absorbance (extinction) vs. time data points by the described eqn (1) (see text). The kinetic parameters,  $k$  and  $n$ , were obtained by nonlinear least-squares regression fit (Kaleidagraph<sup>®</sup> program, Synergy Software, 2003) over hundreds of experimental data points. The results were run in duplicate, with uncertainties within 5%. The quality of the fit is generally very good, with  $R^2 \geq 0.9996$ , and the calculated values for  $Ext_{\infty}$  and  $Ext_0$  are always in excellent agreement with the experimental values. Data reported are the average values of at least two different runs. Analogous experimental protocols have been used in the case of kinetic experiments run at a fixed ionic strength, by replacing the amount of water with a set NaBr solution. It has been reported<sup>17</sup> that the aggregation process can be quite dependent on either the initiation protocol, such as for example the mixing order of solution components, and on the ageing of the porphyrin stock solutions. In our cases, using freshly prepared solutions and the same order of mixing ensures good reproducibility. However, different mixing protocols gave similar results, although of lower reproducibility, in terms of kinetic parameter values.

### CD spectroscopic studies

CD spectra were obtained on a JASCO J-600, equipped with a thermostated cell holder, and purged with ultra-pure nitrogen gas.

### Resonance light scattering experiments

RLS experiments were performed on a Spex Fluorolog Fluorimeter. Spectra were acquired at  $25.0 \pm 0.5$  °C in a “synchro-scan” mode, in which the emission and excitation monochromators are pre-set to identical wavelengths. Solutions were prepared by following the protocol used in the UV-visible aggregation studies.

### Fluorescence spectroscopy experiments

Fluorescence excitation spectra were recorded at  $25.0 \pm 0.5$  °C on a Spex Fluorolog Fluorimeter.

## Acknowledgements

This work was supported by the NATO grant CBP.EAP. CLG.982972, and the Ministry of Education, Youth and Sports of the Czech Republic projects No. MSM6046137305, 203/06/0006, OC08043 (NPFM-II), 2B06024 (SUPAFYT). We thank MIUR-FIRB, Italy (Project nr. RBNE01KZZM) for financial support.

## References

- (a) *Supramolecular Chirality. Topics in Current Chemistry*, eds. M. Crego-Calama and D. N. Reinhoudt, Springer, New York, 2006, vol. 265; (b) M. A. Mateos-Timoneda, M. Crego-Calama and D. N. Reinhoudt, *Chem. Soc. Rev.*, 2004, **33**, 363–372.
- J. Zhang, M. T. Albelda, Y. Liu and J. W. Canary, *Chirality*, 2005, **17**, 404–420, and references therein.
- R. Paolesse, D. Monti, L. La Monica, M. Venanzi, A. Froiio, S. Nardis, C. Di Natale, E. Martinelli and A. D'Amico, *Chem.–Eur. J.*, 2002, **8**, 2476–2483.
- (a) R. F. Pasternack, E. J. Gibbs, P. J. Collings, J. C. dePaula, L. C. Turzo and A. Terracina, *J. Am. Chem. Soc.*, 1998, **120**, 5873–5878; (b) R. F. Pasternack, E. J. Gibbs, D. Bruzewicz, D. Stewart and K. S. Engstrom, *J. Am. Chem. Soc.*, 2001, **124**, 3533–3539; (c) E. Bellacchio, R. Lauceri, S. Guerrieri, L. Monsù Scolaro, A. Romeo and R. Purrello, *J. Am. Chem. Soc.*, 1998, **120**, 12353–12354; (d) R. Purrello, A. Raudino, L. Monsù Scolaro, A. Loisi, E. Bellacchio and R. Lauceri, *J. Phys. Chem. B*, 2000, **104**, 10900–10908; (e) R. Lauceri, A. Raudino, Monsù Scolaro, N. Micali and R. Purrello, *J. Am. Chem. Soc.*, 2002, **124**, 894–895; (f) M. Balaz, M. De Napoli, A. E. Holmes, A. Mammanna, K. Nakanishi, N. Berova and R. Purrello, *Angew. Chem., Int. Ed.*, 2005, **44**, 4006–4009; (g) A. Mammanna, A. D'Urso, R. Lauceri and R. Purrello, *J. Am. Chem. Soc.*, 2007, **129**, 8062–8063, and references therein.
- (a) V. Král, F. P. Schmidtchen, K. Lang and M. Berger, *Org. Lett.*, 2002, **4**, 51–54; (b) S. Muniappan, S. Lipstman and I. Goldberg, *Chem. Commun.*, 2008, 1777–1779, and references therein.
- (a) V. V. Borovkov, G. A. Hembury and Y. Inoue, *Acc. Chem. Res.*, 2004, **37**, 449–459; (b) V. Borovkov, T. Harada, G. A. Hembury, Y. Inoue and R. Kuroda, *Angew. Chem., Int. Ed.*, 2003, **42**, 1746–1749; (c) V. Borovkov, T. Harada, G. A. Hembury and Y. Inoue, *Angew. Chem., Int. Ed.*, 2003, **42**, 5310–5314; (d) G. Pescitelli, S. Gabriel, Y. Wang, J. Fleischhauer, R. W. Woody and N. Berova, *J. Am. Chem. Soc.*, 2003, **125**, 7613–7626; (e) H. Ishii, Y. Chen, R. A. Miller, S. Karady, K. Nakanishi and N. Berova, *Chirality*, 2005, **17**, 305–315; Y. Kubo, Y. Ishii, T. Yoshizawa and S. Tokita, *Chem. Commun.*, 2004, 1394–1395; (f) D. Monti, L. La Monica, A. Scipioni and G. Mancini, *New J. Chem.*, 2001, **25**, 780–781; (g) Y. Kubo,

- Y. Ishii, T. Yoshizawa and S. Tokita, *Chem. Commun.*, 2004, 1394–1395; (h) Y. Ishii, Y. Soeda and Y. Kubo, *Chem. Commun.*, 2007, 2953–2955.
- 7 (a) R. Rubires, J.-A. Farrera and J. M. Ribó, *Chem.–Eur. J.*, 2001, **7**, 436–446; (b) J. M. Ribó, J. Crusats, F. Sagués, J. M. Claret and R. Rubires, *Science*, 2001, **292**, 2063–2066; (c) J. Crusats, J. M. Claret, I. Diez-Pérez, Z. El-Hachemi, X. García-Ortega, R. Rubires, F. Sagués and J. M. Ribó, *Chem. Commun.*, 2003, 1588–1589.
- 8 (a) Y. Zhang, P. Chen and M. Liu, *Chem.–Eur. J.*, 2008, **14**, 1793–1803; (b) Z. Guo, J. Yuan, Y. Cui, F. Chang, W. Sun and M. Liu, *Chem.–Eur. J.*, 2005, **11**, 4155–4162; (c) P. Chen, X. Ma, P. Duan and M. Liu, *ChemPhysChem*, 2006, **7**, 2419–2423.
- 9 (a) J. Charvátová, O. Rusin, V. Král, K. Volka and P. Matějka, *Sens. Actuators, B*, 2001, **76**, 366–372; (b) N. Solladie, M. Gross, J.-P. Gisselbrecht and C. Soombar, *Chem. Commun.*, 2001, 2206–2207; (c) M. Dukh, D. Šaman, K. Lang, V. Pouzar, I. Černý, P. Drašar and V. Král, *Org. Biomol. Chem.*, 2003, **1**, 3458–3463; (d) K. Zelenka, T. Trnka, I. Tišlerová, V. Král, M. Dukh and P. Drašar, *Collect. Czech. Chem. Commun.*, 2004, **69**, 1149–1160; (e) M. Dukh, P. Drašar, I. Černý, V. Pouzar, J. A. Shriver, V. Král and J. L. Sessler, *Supramol. Chem.*, 2002, **14**, 237–244.
- 10 (a) D. Monti, M. Venanzi, M. Stefanelli, A. Sorrenti, G. Mancini, C. Di Natale and R. Paolesse, *J. Am. Chem. Soc.*, 2007, **129**, 6688–6689; (b) D. Monti, M. Venanzi, M. Mancini, C. Di Natale and R. Paolesse, *Chem. Commun.*, 2005, 2471–2473; (c) D. Monti, V. Cantonetti, M. Venanzi, C. Bombelli, F. Ceccacci and G. Mancini, *Chem. Commun.*, 2004, 972–973.
- 11 P. Štěpánek, M. Dukh, D. Šaman, J. Moravcová, L. Kniežo, D. Monti, M. Venanzi, G. Mancini and P. Drašar, *Org. Biomol. Chem.*, 2007, **5**, 960–970.
- 12 S. E. Kiehna, Z. R. Laughrey and M. L. Waters, *Chem. Commun.*, 2007, 4026–4028, and references therein.
- 13 C. Schell and H. K. Hombrecher, *Chem.–Eur. J.*, 1999, **5**, 587–598.
- 14 K. Kano, K. Fukuda, H. Wakami, R. Nishiyabu and R. F. Pasternack, *J. Am. Chem. Soc.*, 2000, **122**, 7494–7502.
- 15 The minimum number of electronically interacting porphyrin chromophores, to give RLS signals, has been calculated to be 25. An RLS intensity with order of magnitude of  $10^7$ – $10^8$  cps should be consistent to aggregated structures composed by  $10^4$ – $10^5$  units. See, for example: (a) R. F. Pasternack and P. J. Collings, *Science*, 1995, **269**, 935–939; (b) R. F. Pasternack, C. Bustamante, P. J. Collings, A. Giannetto and E. J. Gibbs, *J. Am. Chem. Soc.*, 1993, **115**, 5393–5399; (c) J. Parkash, J. H. Robblee, J. Agnew, E. Gibbs, P. Collings, R. F. Pasternack and J. C. de Paula, *Biophys. J.*, 1998, **74**, 2089–2099.
- 16 (a) M. A. Castriciano, A. Romeo and L. Monsù Scolaro, *J. Porphyrins Phthalocyanines*, 2002, **6**, 431–438; (b) The term *Extinction* is of more correct use than the term *Absorbance*, owing to the contribution of the RLS component in the UV-visible and CD spectral bands. For a discussion on this topic, see: N. Micali, F. Mallamace, M. Castriciano, A. Romeo and L. Monsù Scolaro, *Anal. Chem.*, 2001, **73**, 4958–4963.
- 17 R. F. Pasternack, C. Fleming, S. Herring, P. J. Collings, J. dePaula, G. DeCastro and E. J. Gibbs, *Biophys. J.*, 2000, **79**, 550–560.
- 18 (a) N. Micali, F. Mallamace, A. Romeo, R. Purrello and L. Monsù Scolaro, *J. Phys. Chem. B*, 2000, **104**, 5897–5904; (b) L. Monsù Scolaro, M. Castriciano, A. Romeo, A. Mazzaglia, F. Mallamace and N. Micali, *Physica A*, 2002, **304**, 158–169; (c) F. Mallamace, L. Monsù Scolaro, A. Romeo and N. Micali, *Phys. Rev. Lett.*, 1999, **82**, 3480–3483.
- 19 (a) J. C. dePaula, J. H. Robblee and R. F. Pasternack, *Biophys. J.*, 1995, **68**, 335–341; (b) R. F. Pasternack, J. I. Goldsmith, S. Szép and E. J. Gibbs, *Biophys. J.*, 1998, **75**, 1024–1031.
- 20 (a) T. S. Balaban, N. Berova, C. M. Drain, R. Hauschild, X. Huang, H. Kalt, S. Lebedkin, J.-M. Lehn, F. Nifaitis, G. Pescitelli, V. Prokhorenko, G. Riedel, G. Smeureanu and J. Zeller, *Chem.–Eur. J.*, 2007, **13**, 8411–8427; (b) T. S. Balaban, *Acc. Chem. Res.*, 2005, **38**, 612–623; T. S. Balaban, M. Linke-Schaetzel, A. D. Bhise, N. Vanthuyne, C. Roussel, C. E. Anson, G. Buth, A. Eichhöfer, K. Foster, G. Garab, H. Gliemann, R. Goddard, T. Javorfi, A. K. Powell, H. Rösner and T. Schimmel, *Chem.–Eur. J.*, 2005, **11**, 2267–2275; (c) T. S. Balaban, A. D. Bhise, M. Fisher, M. Linke-Schaetzel, C. Roussel and N. Vanthuyne, *Angew. Chem., Int. Ed.*, 2003, **42**, 2140–2144; (d) V. Cantonetti, D. Monti, M. Venanzi, C. Bombelli, F. Ceccacci and G. Mancini, *Tetrahedron: Asymmetry*, 2004, **15**, 1969–1977; (e) D. Monti, P. Tagliatesta, G. Mancini and T. Boschi, *Angew. Chem., Int. Ed.*, 1998, **37**, 1131–1133; (f) F. J. M. Hoeben, M. Wollfs, J. Zhang, S. De Feyter, P. Lacièrre, A. P. H. J. Schenning and E. W. Meijer, *J. Am. Chem. Soc.*, 2007, **129**, 9819–9828; (g) a supramolecular artificial photosynthetic mimic, based on a helical amylose as host for a dye aggregation, has recently published. See O.-K. Kim, J. Melinger, S.-J. Chung and M. Pepitone, *Org. Lett.*, 2008, **10**, 1625–1628.
- 21 J. A. A. W. Elemans, R. van Hameren, R. J. M. Nolte and A. E. Rowan, *Adv. Mater.*, 2006, **18**, 1251–1266.
- 22 (a) R. Purrello, S. Guerrieri and R. Lauceri, *Coord. Chem. Rev.*, 1999, **190–192**, 683–706; (b) L. S. Dolci, E. Marzocchi, M. Montalti, L. Prodi, D. Monti, C. Di Natale, A. D'Amico and R. Paolesse, *Biosens. Bioelectron.*, 2006, **22**, 399–404; (c) Y. Miura, T. Yamauchi, H. Sato and T. Fukuda, *Thin Solid Films*, 2008, **515**, 2443–2449.
- 23 T. Mallat, E. Orglmeister and A. Baiker, *Chem. Rev.*, 2007, **107**, 4863–4890.
- 24 (a) S. E. Wolf, N. Loges, B. Mathiasch, M. Panthöfer, I. Mey, A. Janshoff and W. Tremel, *Angew. Chem., Int. Ed.*, 2007, **46**, 5618–5613; (b) L. Addadi and S. Weiner, *Nature*, 2001, **411**, 753–755; (c) A. R. A. Palmans and E. W. Meijer, *Angew. Chem., Int. Ed.*, 2007, **46**, 8948–8968.